Title Page

Phospholipid component defines pharmacokinetic and pharmacodynamic properties of synthetic high-density lipoproteins

Maria V. Fawaz[1][*], Sang Yeop Kim[2][*], Dan Li[2], Ran Ming[2], Ziyun Xia[2], Karl Olsen[2], Irina D. Pogozheva[1], John J. G. Tesmer[3] and Anna Schwendeman[2,5][**]

*Denotes equal contribution

[1]Department of Medicinal Chemistry, College of Pharmacy, University of Michigan, Ann Arbor, MI 48109

[2]Department of Pharmaceutical Sciences, College of Pharmacy, University of Michigan, Ann Arbor, MI 48109

[3]Department of Biological Sciences, Purdue University, West Lafayette, IN 47907

[5]Biointerfaces Institute, University of Michigan, Ann Arbor, MI 48109

Running title: Phospholipid component defines PK and PD properties of sHDL

**Corresponding author

Anna Schwendeman

Department of Pharmaceutical Sciences

University of Michigan College of Pharmacy

B20-102W NCRC, 2800 Plymouth Road,

Ann Arbor, MI 48109

Phone: +1 734 763 4056

Fax: +1 734 615 6162

E-mail address: annaschw@med.umich.edu

# of text pages: 35

# of tables: 3 (and 2 supplemental table)

# of figures: 6

# of references: 53

# of words in abstract: 219

# of words in introduction: 717

# of words in discussion: 1092

Abbreviations: ABCA1, ATP-binding cassette transporter A1; ApoA-I, apolipoprotein A-I; DLS,

dynamic light scattering; DMPC, 1,2-dimyristoyl-*sn*-glycero-3-phosphocholine; DPPC, 1,2-

dipalmitoyl-*sn*-glycero-3-phosphocholine; DSPC, 1,2-distearoyl-*sn*-glycero-3-phosphocholine;

EC, esterified cholesterol; FC, free cholesterol; LCAT, lecithin:cholesterol acyltransferase; PD,

pharmacodynamic; PK, pharmacokinetic; PL, phospholipid; POPC, 1-palmitoyl-2-oleoyl-*sn*-

glycero-3-phosphocholine; RCT, reverse cholesterol transport; sHDL, synthetic high-density

lipoprotein; SR-BI, scavenger receptor class B type I; TC, total cholesterol; Tm, transition

temperatures.

Recommended section assignment: Cardiovascular

Abstract

Synthetic high-density lipoprotein (sHDL) nanoparticles composed of apolipoprotein A-I (ApoA-I) mimetic peptide and phospholipids have been shown to reduce atherosclerosis in animal models. Cholesterol is mobilized from atheroma macrophages by sHDL into the blood compartment and delivered to the liver for elimination. Historically, sHDL drug discovery efforts were focused on optimizing peptide sequences for interaction with cholesterol cellular transporters rather than understanding how both sHDL components, peptide and lipid, influence its pharmacokinetics (PK) and pharmacodynamic (PD) profiles. We designed two sets of sHDL having either identical phospholipid but variable peptide sequences with different plasma stability, or identical peptide and phospholipids with variable fatty acid chain length and saturation. We found that sHDL prepared with proteolytically stable 22A-P peptide had 2-fold longer circulation half-time relative to the less stable 22A peptide. Yet, longer half-life did not translate into any improvement in cholesterol mobilization. In contrast, sHDL with variable phospholipid compositions showed significant differences in phospholipid PK, with distearoyl phosphatidylcholine-based sHDL demonstrating the longest half-life of 6.0 h relative to 1.0 h for palmitoyl-oleoyl phosphatidylcholine-based sHDL. This increase in half-life corresponded to a ~6.5-fold increase in the area under the curve for the mobilized cholesterol. Therefore, the phospholipid component in sHDL plays a major role in cholesterol mobilization *in vivo* and should not be overlooked in the design of future sHDL.

Significance Statement: The phospholipid composition in sHDL plays a critical role in determining half-life and cholesterol mobilization *in vivo.*

Introduction

Reverse cholesterol transport (RCT) is a mechanism of cholesterol removal from the periphery to the liver for elimination. This transport starts when lipid-poor apolipoprotein A-I (ApoA-I) facilitates extracellular efflux of phospholipids and cholesterol through the transmembrane ATP-binding cassette transporter A1 (ABCA1) resulting in formation of pre-β high-density lipoprotein (HDL) particles. Then, pre-β HDLs interact with lecithin:cholesterol acyltransferase (LCAT), an enzyme responsible for cholesterol esterification, leading to formation of larger mature HDLs. Mature HDLs can either deliver esterified cholesterol (EC) cargo directly to the liver for elimination through scavenger receptor class B type I (SR-BI) or transfer EC to LDL by interaction with cholesterol ester transfer protein (CETP) for the elimination by the liver following LDL receptor-mediated uptake.

The idea of using reconstituted (rHDL) or synthetic (sHDL) HDL for the treatment of cardiovascular disease has been prominent in the past 20 years, with several therapies reaching clinical trials (Nissen *et al.*, 2003; Tardif *et al.*, 2007; Tricoci *et al.*, 2015; Duffy, 2018). While some clinical trials for rHDL products were successful (Nissen *et al.*, 2003; Tardif *et al.*, 2007; Duffy, 2018), others failed (Andrews *et al.*, 2017; Nicholls *et al.*, 2018). A 17,400-patient Phase 3 trial (AEGIS-II) is currently ongoing for CSL-112 to show possible reduction of major adverse cardiovascular events in subjects with acute coronary syndrome (Duffy, 2018). The two most advanced sHDL products, CSL-112 and CER-001, both contain ApoA-I but differ in their lipid composition. CSL-112 is prepared from unsaturated soybean phosphatidylcholine while CER-001 is composed of primarily saturated sphingomyelin (Andrews *et al.*, 2017). Recently, we have shown that the type of phospholipid used in sHDL preparation is critical for its anti-inflammatory and anti-atherosclerotic properties (Schwendeman *et al.*, 2015). Several other studies had examined the effects of phospholipid composition on the ability of sHDL to efflux cholesterol and interact with LCAT *in vitro* (Davidson *et al.*, 1995; Bolin and Jonas, 1996; Sparks *et al.*, 1998), yet

the impact of phospholipid chain length and saturation on sHDL pharmacodynamics *in vivo* has not been systematically examined.

In contrast, significant body of research had been performed to develop short peptides (2F (18A), D-4F, L-4F, 5A, 22A, and ATI-5261) as cost-efficient, safe and easily scalable alternatives to a full-length ApoA-I (Dasseux *et al.*, 1999; Remaley *et al.*, 2001; Miles *et al.*, 2004; Navab, GM Anantharamaiah, *et al.*, 2005; Navab, GMM Anantharamaiah, *et al.*, 2005; Sethi *et al.*, 2008; Wool *et al.*, 2008; Vecoli *et al.*, 2011). These ApoA-I mimetic peptides have been optimized with the goal to improve several properties such as ABCA1 mediated cholesterol efflux, ability to activate LCAT and facilitate cholesterol esterification, enhance anti-oxidant properties, improve chemical stability and reduce hemolytic side-effects (Dasseux *et al.*, 1999; Amar *et al.*, 2010; Bielicki *et al.*, 2010; Li *et al.*, 2015). Most ApoA-I mimetics were optimized as "naked" or lipid-free peptides *in vitro* and *in vivo* and only a few studies examined the pharmacological activity of peptide-based sHDL (Amar *et al.*, 2010; Tang *et al.*, 2017).

Thus, we decided to systematically evaluate the effect of both peptide sequence and phospholipid composition of sHDL on nanoparticle's ability to mobilize and esterify cholesterol *in vitro* and *in vivo*. For our studies, we used the first ApoA-I mimetic peptide (22A) that reached clinical trials as part of the sHDL product called ETC-642 (Khan *et al.*, 2003; Miles *et al.*, 2004). ETC-642 contained 22A ApoA-I mimetic peptide, which was optimized for its ability to bind phospholipids and activate LCAT (Dasseux *et al.*, 1999; Di Bartolo *et al.*, 2011). While ETC-642 successfully completed single and multiple dose trials in dyslipidemia patients, it was recently discovered by us that 22A peptide undergoes rapid hydrolysis in plasma to form the 21A peptide, which lacks the C-terminal lysine, a residue potentially important for LCAT activation (Navab *et al.*, 2006; Tang *et al.*, 2017). We hypothesized that the addition of a proline moiety after the labile lysine (22A-P) would be able to protect 22A from proteolysis and result in longer circulation time while retaining LCAT activity *in vivo*. Thus, we prepared a set of sHDL particles using 22A, 21A, and 22A-P peptides while keeping lipid composition constant.

The second set of sHDL was prepared by varying only the phospholipid component and keeping the peptide component, 22A, constant. We used phospholipids with different chain length and saturation including 1-palmitoyl-2-oleoyl-*sn*-glycero-3-phosphocholine (POPC), 1,2-dimyristoyl-*sn*-glycero-3-phosphocholine (DMPC), 1,2-dipalmitoyl-*sn*-glycero-3-phosphocholine (DPPC) or 1,2-distearoyl-*sn*-glycero-3-phosphocholine (DSPC) known for their differences in cholesterol binding affinity and LCAT interaction (Assmann *et al.*, 1978; Subbaiah *et al.*, 1992; Ramstedt and Slotte, 1999). Phospholipids with longer, saturated fatty acid chains such as DPPC and DSPC have higher affinity for cholesterol binding and higher physical stability due to their high transition temperatures (T_m) of 41°C and 55°C, respectively (Small, 1986; Ramstedt and Slotte, 1999; Ohvo-Rekilä *et al.*, 2002). In contrast, unsaturated phospholipids like POPC (T_m= -2°C) and those with shorter fatty acid chains like DMPC (T_m = 23°C) form fluid bilayers at physiological temperature facilitating LCAT-sHDL binding. The unsaturated fatty acids are superior substrates for LCAT esterification activity (Assmann *et al.*, 1978; Parks and Gebre, 1997). By comparing two sets of sHDL with varying peptide and lipid components side by side, we expected to be able to elucidate the relative contribution of both components to cholesterol efflux and engagement of LCAT *in vitro* as well as the overall pharmacokinetic and pharmacodynamic behavior of sHDL *in vivo*.

Materials and Methods

Materials

22A (PVLDLFRELLNELLEALKQKLK), 21A (PVLDLFRELLNELLEALKQKL), and 22AP (PVLDLFRELLNELLEALKQKLKP) were synthesized by Genscript (Piscataway, NJ), using solid-phase Fmoc (9-fluorenylmethyl carbamate) protection chemistry and purified with reverse phase chromatography (>95% pure). 5A peptide (DWLKAFYDKVAEKLKEAF-P-DWAKAAYDKAAEKAKEAA) was obtained from Bachem Americas Inc (Torrance, CA). Phospholipids including 1,2-dimyristoyl-*sn*-glycero-3-phosphocholine (DMPC), 1,2-dipalmitoyl-*sn*-glycero-3-phosphocholine (DPPC), 1,2-distearoyl-*sn*-glycero-3-phosphocholine (DSPC), and 1-palmitoyl-2-oleoyl-*sn*-glycero-3-phosphocholine (POPC) were purchased from NOF America Corporation. Ergosta-5,7,9(11), 22-tetraen-3β-ol (dehydroergosterol, DHE), cholesterol oxidase was obtained from Sigma-Aldrich (St. Louis, MO). Cholesterol (1,2-^{3}H(N)] was purchased from Perkin Elmer. Anti-human ApoA-I horseradish peroxidase-conjugated (HRP) antibody (1:1000 dilution) was purchased from Meridian Life Science (Memphis, TN). Recombinant human lecithin cholesterol acyl transferase (LCAT) was kindly provided by MedImmune (Gaithersburg, MD). All other materials were obtained from commercial sources.

Preparation and characterization of synthetic high-density lipoproteins

sHDL composed of a peptide (22A, 21A, or 22A-P) and phospholipid (DMPC, POPC, DPPC, or DSPC) were prepared by a co-lyophilization procedure (Schwendeman *et al.*, 2015). Briefly, peptide and phospholipids were dissolved in glacial acetic acid, mixed at 1:2 w/w ratio of peptide:lipid, and lyophilized overnight. The powder was hydrated with PBS pH 7.4 to make 10 mg/mL sHDL and cycled between 55°C (10 min) and room temperature (10 min) to facilitate sHDL formation. The resulting sHDL complexes were analyzed by gel permeation chromatography for purity at 1 mg/mL using a 7.8 mm x 30 cm Tosoh TSK gel G3000SWxl column (Tosoh Bioscience, King of Prussia, PA) with UV detection at 220 nm. The HDL hydrodynamic diameters were

8

determined by dynamic light scattering (DLS) using a Zetasizer Nano ZSP, Malvern Instruments (Westborough, MA). The volume intensity average values were reported. The α-helical content of free and lipid-bound peptide was determined by Jasco J715 (Jasco, Easton, MD) circular dichroism (CD) spectropolarimeter. Samples at 0.1 mg/mL concentration in 10 mM phosphate buffer (pH 7.4) or buffer alone were loaded into a quartz cuvette (d = 0.2-cm path length), and CD spectra from 190 to 260 nm were recorded at 37°C. Buffer spectra were subtracted from each peptide or sHDL sample. Data analysis was conducted using CDPro analysis software and the percent helical content for each sample was calculated via CONTIN analysis method with the reference Soluble–Membrane Protein 56 Data Base (Sreerama and Woody, 2000).

Generation of helical wheel peptide models and calculation of lipid binding parameters

Helical wheel plots of 22A, 21A, and 22A-P peptides were created by Helixator (http://tcdb.org/progs/helical_wheel.php). This program displayed a peptide sequence looking down the axis of the alpha helix with aliphatic residues shown as blue circles. The hydrophobic momentum of 22A, 21A, and 22A-P peptides was calculated using the 3D Hydrophobic Moment Vector Calculator (http://www.ibg.kit.edu/HM/) (Reißer *et al.*, 2014). The helix stability (ΔG_{hel}), transfer energy from water to membrane (ΔG_{trans}), and parameters of spatial positions in membranes (tilt angle and membrane penetration depth) for each ApoA-I-mimetic peptide were calculated by the Folding of Membrane-Associated Peptide (FMAP) server (Lomize *et al.*, 2017) and the Positioning of Proteins in Membranes (PPM) server (Lomize *et al.*, 2012).

Cholesterol efflux assay *in vitro*

Cholesterol efflux studies were performed, as described by Remaley *et al.* (Remaley *et al.*, 2003). Briefly, RAW 264.7, BHK-Mock and BHK stably transfected with human ABCA1 cDNA cell lines were labeled for 24 h with 1 μCi/mL of [³H] cholesterol in minimum Dulbecco's modified Eagle's medium (DMEM), containing 0.2 mg/ml of fatty acid-free bovine serum albumin (BSA).

Then, BHK-MOCK and BHK-ABCA1 cell lines were treated with 10 nM mifepristone for 18 h to selectively induce the expression of ABCA1 cholesterol transporter for BHK-ABCA1. ABCA1 transporter was not selectively induced in RAW 264.7 cell line. Following the radiolabeling or induction step, peptides (22A, 21A or 22A-P) or sHDL (21A-DMPC, 22A-P-DMPC, 22A-DMPC, 22A-POPC, 22A-DPPC or 22A-DSPC) were added at 0.01, 0.03 and 0.1 mg/mL concentration using DMEM-BSA media. After 18 h of incubation with cholesterol acceptors, media were collected and cells were lysed in 0.5 ml of 0.1% SDS and 0.1 N NaOH for 2 h. Radioactive counts in media and cell fractions were measured by liquid scintillation counting (Tri-Carb 2910 TR, PerkinElmer), and percent cholesterol efflux was calculated by dividing media counts by the sum of media and cell counts.

Phospholipid lipolysis by LCAT

The rate of phospholipid (POPC, DMPC, DPPC or DSPC) lipolysis was evaluated by incubating 15 μg/mL of rhLCAT with 0.1 mg/mL of sHDL (based on total lipid concentration) in 0.1 M sodium phosphate buffer pH 7.4 for 0, 5, 15, 30, 60, 90, and 120 min. The LCAT-sHDL reaction aliquots were collected into methanol (1:5 v/v) and vortexed to stop the lipolysis reaction at each time point. The amount of POPC, DMPC, DPPC or DSPC remaining at each time point was measured by Waters UPLC-MS equipped with QDa Mass Detector (Milford, MA). Chromatographic separation was achieved on Acquity BEH300 1.7 μm HILIC 2.1 x 50 mm column with gradient elution at 0.65 mL/min: mobile phase A (H$_2$O/0.1% formic acid), mobile phase B (acetonitrile/0.1% formic acid) and mobile phase C (100 mM ammonium formate) as follows: 0-0.7 min (5-17% A, 90-78% B, and 5-5% C), 0.7-0.71 min (17-5% A, 78-90% B, and 5-5% C), and 0.71-3 min (17-5% A, 78-90% B, and 5-5% C). Mass spectra were acquired in the positive ion mode with the mass range set at m/z 150-1250 and POPC was detected at 760.7 amu, DMPC at 678.7 amu, DPPC at 734.7 amu, and DSPC at 790.7 amu. Data analysis was performed with

Waters Empower software. The plot of POPC, DMPC, DPPC or DSPC area under the curve over time was generated for each sHDL sample. The rate of LCAT lipolysis (k) was calculated from the linear slope of the log10 (concentration) versus time.

Cholesterol esterification by LCAT assay

Two different sets of sHDL containing dehydroergosterol (DHE) was prepared via the thin-film method. Briefly, the first set was made from POPC, DPPC and DHE combined at a 4.5:4.5:1 molar ratio in chloroform and then mixed with peptide (22A, 21A or 22A-P) at 2:1 lipid:peptide weight ratio in methanol/water (4:3 v/v). The second set was prepared from POPC, DMPC, DPPC or DSPC and DHE at a 9:1 molar ratio then mixed with 22A peptide at 2:1 lipid:peptide weight ratio in methanol/water (4:3 v/v). The solvent was removed under nitrogen flow at room temperature and then in a vacuum oven overnight. The lipid film was hydrated with 20 mM phosphate buffer containing 1mM EDTA (pH 7.4) followed by 5 min water bath sonication at room temperature and probe sonication (2 min × 50 w) to obtain clear DHE-sHDL. The final DHE concentration in peptide-DHE-sHDL was 0.5 mM. The LCAT assay was adapted from Homan *et al.* (Homan *et al.*, 2013) and performed in 384-well black polystyrene plates in triplicate. Briefly, 8 μL of different concentrations (0, 5, 10, 20, 40, 60, and 100 μM) of DHE-sHDL (substrates) in assay buffer (PBS containing 1 mM EDTA, 5 mM β-mercaptoethanol, and 60 μM albumin, pH 7.4) preheated to 37°C were incubated with 8 μL of 5 μg/mL LCAT in dilution buffer (PBS with 1 mM EDTA and 60 μM albumin, pH 7.4) preheated to 37°C in triplicates. The plates were incubated at 37°C with gentle shaking (80 rpm/min) for different lengths of time (0, 10, and 20 min). Reactions were stopped by adding 4 μL of stop solution (3.75 U/mL cholesterol oxidase) in PBS containing 1mM EDTA and 7% Triton X-100. Then, the plates were incubated at 37°C with shaking (80 rpm/min) for another 1 h to quench the fluorescence of unesterified DHE. The fluorescence was measured at an excitation wavelength of 325 nm and an emission wavelength of 425 nm using the plate-reader (SynergyTM NEO HTS Multi-Mode Microplate Reader, Bio-Tek). A standard

11

curve was made by plotting the fluorescence of serially diluted DHE-containing sHDL mixed with

LCAT and using stop solution without COx versus the concentration (μM) of DHE. To calculate

the concentration (μM) of DHE ester for each reaction, the background fluorescence (0 μM of

DHE) was subtracted from all fluorescence measurements and then divided by the slope

(fluorescence/μM) of the above standard curve. To calculate V_{max} and K_m, the concentrations (μM)

of DHE ester at different time points were plotted against time (h), and the initial velocity (V_0, μM

DHE-ester/h) was the slope of the linear range of DHE-ester concentration versus time. The V_{max}

and K_m were obtained by plotting V_0 versus DHE concentration and then analyzed by GraphPad

Prism 7 (nonlinear regression, Michaelis-Menten model).

Plasma peptide stability

The *in vitro* stability of 22A, 21A, and 22A-P peptides was assessed by the addition of 2.5

μL of 10 mg/mL of a peptide to 97.5 μL of fresh rat plasma (K2 EDTA, Innovative Research Inc).

Immediately after the addition of peptide to plasma, 10 μL of serum was removed to serve as a

baseline and stored at -20 °C. Samples were incubated at 37°C for 24 hours with shaking at 240

rpm. To determine peptide concentration at 0 and 24 h post plasma incubation, 10 μL of plasma

containing a peptide or working standard (0-100 μg/mL) was mixed with 2 μL of 2.4 mg/mL internal

standard (5A peptide) and 38 μL of H_2O. Methanol (200 μL) was added to precipitate plasma

proteins. The mixture was vortexed for 10 s, centrifuged at 12,000 rpm for 10 min and the

supernatant was collected for LC-MS analysis. Samples were mixed (1:1 v/v) with LC-MS mobile

phase (80:20 v/v H_2O:acetonitrile, 0.1% formic acid) and analyzed on Waters Acquity UPLC

equipped with QDa System (Milford, MA) using Acquity UPLC BEH C18 1.7 μM column for

separation. The mobile phase consisted of (A) water containing 0.1% v/v formic acid and (B)

methanol containing 0.1% v/v formic acid. The mobile phase was delivered at 0.3 mL/min using

a gradient elution of 20% to 80% B during 0-1.5 min, and 80% to 20% B during 1.5-3.5 min. Mass

spectra were acquired in the positive ion mode with the mass range set at m/z 150-1250. Data

analysis was performed on Waters Empower software. The concentration of 22A, 21A or 22A-P peptide in each sample was determined from the standard curve.

Peptide pharmacokinetics, cholesterol mobilization, and esterification *in vivo*

Healthy male Sprague-Dawley rats (8 weeks old) were purchased from Charles River Breeding Laboratories (Portage, MI) and were fed a standard rodent chow diet. To examine the impact of peptide composition on sHDL PK/PD properties, animals were randomly assigned to two groups (n = 4/group) for 22A-POPC/DPPC and 22A-P- POPC/DPPC administration. To examine the impact of lipid composition on sHDL PK/PD, animals were randomly assigned to four groups (n = 3/group) for 22A-POPC, 22A-DMPC, 22A-DPPC, and 22A-DSPC administration. All sHDL particle was prepared at 1:2 w/w peptide to phospholipid ratios, sterile filtered and characterized by DLS and gel permeation chromatography for size and purity prior to animal dosing. All animals were fasted overnight before sHDL dosing at 50 mg/kg (based on peptide concentration) via tail vein injection. At each time point (pre-dose, 0.25, 0.5, 1, 2, 4, 8, and 24 h) blood samples (~0.3 mL) were collected from the jugular vein to heparinized BD tubes (Franklin Lakes, NJ) and centrifuged at 10,000 rpm for 10 min at 4°C. The obtained serum samples were stored at -20°C for further analysis.

The levels of plasma phospholipids (PL), total cholesterol (TC) and free cholesterol (FC) were determined enzymatically (Wako Chemicals, Richmond, VA) using a plate reader (SynergyTM NEO HTS Multi-Mode Microplate Reader, Bio-Tek). Esterified cholesterol levels (EC) were calculated as the difference between TC and FC levels at each time point. Briefly, serum samples were diluted with PBS for TC and FC detection, or with MilliQ water for PL detection. Defined amounts of standards or diluted samples were transferred to 96-well plates (50 μL, 60 μL and 20 μL for TC, FC and PL analyses, respectively), and assay reagents were added per manufacturer's instructions. The plates were gently shaken using an orbital shaker and incubated

13

at 37˚C for 5 minutes. The UV absorbance at 600 nm was measured by a Molecular Devices

SpectraMax M3 plate reader (Sunnyvale, CA). Pharmacokinetic parameters were also obtained

by non-compartmental analysis. The pharmacodynamic effect in each rat was determined as the

area under the total effect curve ($AUEC$) using trapezoidal rule. Secondary pharmacodynamic

endpoints, maximal effect (E_{max}) and time to E_{max} ($T_{max,E}$) were also analyzed to compare

pharmacodynamic effects.

Peptide (22A or 22A-P) concentration in serum was determined by LC-MS. The 10 μL

serum aliquots were combined with 10 μL of 2.4 mg/mL of internal standard (5A peptide) and then

mixed with 40 μL ddH$_2$O. Working standard solutions (0-100 μg/mL) of 22A and 22A-P were

prepared as described above for plasma samples with the exception of using blank rat serum.

Plasma proteins were precipitated by adding 180 μL of methanol. After 5 minutes, the mixture

was centrifuged (12000 rpm × 10 min, 4°C) and 100 μL of the supernatant was used for analysis.

Each sample was analyzed by LC-MS as described above in the plasma peptide stability section.

Pharmacokinetic parameters such as maximum serum concentration (C_{max}), the area under the

serum concentration-time curve (AUC), elimination rate constant (K), elimination half-life ($T_{1/2}$),

total clearance (CL), and volume of distribution (V_d) were obtained by non-compartmental

analysis.

Remodeling of endogenous lipoproteins by sHDL in human plasma

Remodeling of endogenous lipoproteins in human plasma by sHDL was assessed by one-

dimensional native polyacrylamide gel electrophoresis (1-D native PAGE) following sHDL

incubation in plasma. Various sHDL (22A-POPC, 22A-DMPC, 22A-DPPC, 22A-DSPC, 21A-

sHDL, 22A-sHDL, and 22A-P-sHDL) at 1 mg/mL concentration were incubated at 37°C for 1 h

with shaking at 300 rpm. The sub-classes of HDL were separated by size using 1-D native PAGE

and visualized by Western Blot using the anti-ApoA-I antibody. Briefly, samples were subjected

to electrophoresis using Tris-borate-EDTA (TBE) gradient (4 – 20%) acrylamide mini-gels. For

14

each well, 10 μL of human plasma incubated with or without sHDL was mixed with 10 μL of 2X TBE sample buffer, and 6 μL of the resulting mixtures were loaded per well. Gels were run at 200V. Proteins were transferred to polyvinylidene difluoride membrane (PVDF) and incubated overnight with the anti-human ApoA-I-HRP conjugated antibody. Proteins were visualized with the enhanced chemiluminescent substrate on Protein Simple FluorChem M imaging system (San Jose, CA).

Statistical analysis

Significance of difference was determined by Student's *t*-test for comparing two groups or by one-way analysis of variance (ANOVA) with Dunnett's post-hoc test for comparing multiple groups with 22A peptide or 22A-DMPC as the control. All samples were performed in triplicate and error bars were reported as a standard mean error (SEM) unless noted otherwise. $P < 0.05$ was considered statistically significant.

Results

Design of ApoA-I peptides with improved plasma stability

Helical wheel plots for 22A, 22A-P, and 21A were generated to assess the amphipathic nature of each peptide. The hydrophobic amino acids clustered on one side of the helix suggested an amphipathic orientation of each peptide (**Table 1**). The 3D hydrophobic moment vector calculations were performed to predict and compare the interactions of each peptide with lipid membranes. It was determined that the hydrophobic moment vectors were almost identical with an average of 10.3 ± 0.7 A*kT/e. Additionally, we used an online server to determine the helix stability ($\Delta\mathbf{G_{hel}}$), transfer energy from water to membrane ($\Delta\mathbf{G_{trans}}$), and orientation of each peptide in the membrane (penetration depth, D). Again, we did not find large differences in any of the aforementioned parameters, suggesting that the absence of the terminal lysine in 21A or the addition of proline in 22A-P did not change the physical properties of these peptides compared to 22A. Next, we compared the plasma stability of 22A, 22A-P, and 21A as well as their abilities to bind lipid and form sHDL particles. We found that while 22A degrades in plasma with only 48% of intact peptide remaining after 24 h incubation at 37°C, both 22A-P and 21A are significantly more stable with 89 and 97% of intact peptide remaining, respectively. These results suggest that the plasma stability of 22A peptide can be greatly improved by the addition of a bulky proline, while computed lipid binding properties remained relatively unchanged.

Preparation and characterization of sHDL particles

We next evaluated the ability of 21A, 22A, and 22A-P peptide to form homogeneous sHDL particles. Synthetic HDL particles were prepared by combining 22A, 21A or 22A-P peptide with DMPC at 1:2 w/w peptide:lipid ratio, which was previously used in ETC-642 formulation resulting in the formation of homogeneous sHDL particles with approximately 10 nm size (Li *et al.*, 2015; Tang *et al.*, 2017). All three peptides formed homogeneous sHDL particles with average

16

diameters of approximately 10 nm and a narrow polydispersity index of 0.17 ± 0.04 as determined by DLS (**Fig. 1A**). Purity and homogeneity of sHDL size distribution were evaluated by gel permeation chromatography (**Fig. 1B**). All three sHDL were over 98% pure, and negligible levels of the free peptide (<2%) were observed at the retention time of ~11 min (**Supplemental Table 1**). The binding of a peptide to phospholipid was also confirmed by increased helicity of 22A, 21A and 22A-P in sHDL particles (94, 91 and 82%) relative to the free peptide (77, 79 and 77%) as measured by CD.

We also altered the phospholipid composition of 22A sHDL to study its impact *in vitro* and *in vivo*. We chose four lipids with different physical properties such as transition temperature (T_m) and affinity for cholesterol (DSPC>DPPC>DMPC>POPC) (Small, 1986; Ramstedt and Slotte, 1999; Ohvo-Rekilä *et al.*, 2002). The sHDL complexes were formed by combining 22A peptide with individual lipids at 1:2 w/w ratio using the co-lyophilization method. All were highly homogeneous with an average hydrodynamic diameter ranging between 8.3 to 10.5 nm, low polydispersity index and gel permeation chromatography purity greater than 95% (**Fig. 1C-D**). The purity, size, and polydispersity levels of sHDL are summarized in **Supplemental Table 1.** The DMPC, DPPC and DSPC-based sHDL had smaller hydrodynamic diameters, higher GPC purities, and sharper GPC peaks relative to 22A-POPC. The presence of free peptide (<1%, retention time ~11.3 min) and liposome impurities (<2%, retention time ~5.5 min) were observed for 22A-POPC, which also had the largest average particle size and broadest size distribution. Because POPC has the lowest T_m of -2 °C, it exists in a fluid gel state at room temperature, which likely impacts 22A-POPC stability.

Lipid composition of sHDL impacts macrophage cholesterol efflux

We next examined how the C-terminal modifications in 22A-P and 21A impact cholesterol efflux abilities relative to 22A, either as free peptides or reconstituted into sHDL. Radioactive cholesterol was loaded into BHK cell line stably transfected with human ABCA1 transporter and

peptides were incubated with the cells at 0, 0.01, 0.03, and 0.1 mg/mL. The same experiment was repeated using the control BHK-Mock cell line to assess cholesterol efflux by passive diffusion. Then, the non-specific cholesterol efflux values were subtracted from the data obtained for each peptide with ABCA1 transfected cells to reveal receptor specific cholesterol efflux (**Fig. 2A**). All three peptides exhibited concentration-depended cholesterol efflux with only minor differences (< 5%) observed, indicating that modifications at the C terminal end of 22A did not affect lipid binding and ABCA1 transporter interaction. Then, the three peptide sequences were assembled into sHDL and their abilities to efflux cholesterol from macrophages were examined in RAW 264.7 cell line (**Fig. 2B**). Similar to free peptide, we observed concentration-dependent cholesterol efflux with only minor differences (< 5%) at concentrations tested.

To explore the impact of the phospholipid component of sHDL on macrophage cholesterol efflux, 22A-POPC, 22A-DMPC, 22A-DPPC, and 22-DSPC were incubated with RAW 264.7 cells. Saturated long chain length phospholipids such as DPPC and DSPC have higher physical binding affinity to cholesterol relative to POPC and DMPC (Ramstedt and Slotte, 1999; Ohvo-Rekilä *et al.*, 2002). However, the transition temperature of POPC and DMPC is below 37°C, thus the phospholipid bilayer is in liquid crystal state at physiological temperature facilitating cholesterol partitioning in these sHDL particles at the cell culture conditions (Davidson *et al.*, 1995). As expected, we observed greater cholesterol efflux to POPC and DMPC-based sHDL relative to DPPC and DSPC-based sHDL likely due to differences in lipid fluidity at 37°C (**Fig. 2C**). Whereas 22A-DPPC and 22A-DSPC did not have any significant differences in cholesterol efflux as concentration increased, 22A-POPC and 22A-DMPC show sHDL concentration-dependent increase in cholesterol efflux. Interestingly, 22A-DMPC showed the most effective cholesterol efflux capability from as low as 36% at 0.01 mg/mL to as high as 61.8% at 0.1 mg/mL concentration. Membrane transporters such as ABCG1/G4 and SR-BI are known to play a major role in cholesterol efflux to HDL rather than lipid-free protein and may contribute to the differences seen between sHDL in our study (Krieger, 1999; Wang *et al.*, 2004). Taken together, the

phospholipid composition of sHDL appears to play a significant role in cholesterol efflux from macrophages in cell culture.

Peptide and lipid composition both impact sHDL interaction with LCAT

Following cholesterol efflux from macrophages, sHDL particles interact in plasma with LCAT (Asztalos *et al.*, 2007). It is expected that both lipid and peptide composition of sHDL will have an effect on LCAT interaction. The fluidity of HDL lipid membrane determines the ease of LCAT binding to HDL particles (Soutar *et al.*, 1975). It has been shown that LCAT interaction with ApoA-I is critical for LCAT activation, especially for the facilitation of acyltransferase activity (Sorci-Thomas *et al.*, 1993). Whereas some ApoA-I mimetic peptides have similar LCAT activation ability to full-length ApoA-I, others fail to facilitate EC formation (Anantharamaiah *et al.*, 1990; Dasseux *et al.*, 1999; Datta *et al.*, 2001). The presence of positively charged clusters on the C-terminus and presence of hydrophobic amino acids at positions 3, 6, 9 and 10, and net peptide charge of zero are believed to be critical to the high LCAT activation ability of 22A (Dasseux *et al.*, 1999, 2004). To examine how modification of 22A and lipid composition of sHDL impact phospholipase A2 activity of LCAT, sHDL were co-incubated with enzyme and the kinetics of reduction of phospholipid concentration was monitored by LC-MS. We found that small changes in 22A sequence had only limited impact on phospholipase A2 activity (lipolysis) activity (**Fig. 3A**), indicating that LCAT activation by a C-terminal positive cluster on the peptide might not be critical for lipase activity. In contrast, the sHDL lipid composition had profound effect on LCAT-catalyzed phospholipid lipolysis with the rates of 0.08, 0.08, 0.01, and 0.0 h^{-1} for 22A-POPC, 22A-DMPC, 2A-DPPC and 22A-DSPC, respectively. DSPC and DPPC, phospholipids with T_m values above 37°C, had minimal lipolysis likely due to poor LCAT binding to sHDL and, thus, presumably difficulty in the accessibility of substrate for the enzymatic reaction.

Next, we assessed the impact of peptide and lipid composition of sHDL on LCAT acyltransferase activity by incorporating a fluorescent cholesterol analog called dehydroergosterol

and measuring the rate of sterol esterification by LCAT. Changes in C-terminus of 22A peptide had a significant effect on the acyltransferase activity with a 2.6-fold decrease in k_{cat} upon the loss of lysine for 21A (**Fig. 3C**). The rate was only decreased by 30% for 22A-P-HDL. When 22A-sHDL was complexed with different compositions of phospholipids, acyltransferase activity of LCAT was the highest for 22A-POPC sHDL (**Fig. 3D**). Sterol esterification was only limited for 22A-DMPC sHDL, while no activity was detected for 22A-DPPC and 22A-DSPC. This trend was similar to the differences in phospholipase A2 activity observed for sHDL prepared with different lipids (POPC ≥ DMPC > DPPC > DSPC), following their general trends in T_m and membrane fluidity. The Michaelis-Menten parameter estimates for the LCAT assay and goodness of fit are provided in **Supplemental Table 2**. The assay has significant run-to-run variability, however, the samples analyzed within a single experiment (either in **Fig. 3C** or **3D**) can be compared between each other.

Increase in peptide plasma half-life has no impact on cholesterol mobilization *in vivo*

To evaluate whether *in vitro* peptide stability data correlates with *in vivo* peptide pharmacokinetics and cholesterol mobilization, we injected healthy Sprague Dawley rats with 22A-POPC-DPPC or 22A-P-POPC-DPPC sHDL at 50 mg/kg based on peptide concentration in sHDL. Animal blood samples were collected before sHDL administration and at 0.25, 0.5, 1, 2, 4, 8, and 24 h post-dose. The peptide concentrations in rat serum were determined using LC-MS (**Fig. 4A**). The noted stability of 22A-P when incubated with rat plasma translated well to *in vivo* settings with an increase in peptide circulation half-life and exposure ($T_{1/2}$ = 4.2 h and AUC = 1721.0 mg*h/dL) compared to 22A ($T_{1/2}$ = 2.1 h and AUC = 554.0 mg*h/dL) (**Table 2**). We expected that these significant PK differences between two peptides would translate into increased cholesterol mobilization by sHDL *in vivo*. Additionally, we anticipated that levels of esterified cholesterol would be different between two formulations *in vivo* based on clear differences in LCAT-catalyzed esterification between 22A-sHDL and 22A-P-sHDL *in vitro*.

However, we saw no differences in cholesterol mobilization and esterification profiles between 22A-sHDL and 22A-P-sHDL *in vivo* as quantified by enzymatic assay of rat serum samples (**Fig. 4C, D, Table 2**). Finally, if sHDL particle stayed intact upon *in vivo* administration, we would expect to see longer circulation half-life for total phospholipids with 22A-P-sHDL relative to 22A-sHDL. To test this hypothesis, we determined phospholipid concentrations in plasma pre- and post-sHDL administration by an enzymatic assay. We observed no differences in phospholipid PK parameters between 22A-sHDL and 22A-P-sHDL except for $T_{1/2}$ in which 22A-P-sHDL (1.3 h) showed significantly decreased $T_{1/2}$ compared to 22A-sHDL (1.8 h) (**Fig. 4B, Table 2**). Altogether, these results suggest that the apparent differences in 22A-P and 22A stabilities in plasma and LCAT activation abilities had not resulted in measurable differences in cholesterol mobilization and esterification *in vivo*.

Lipid composition of sHDL impacts cholesterol mobilization *in vivo*

To investigate the contribution of phospholipid composition of sHDL on cholesterol mobilization and esterification profiles *in vivo*, we administered 22A-POPC, 22A-DMPC, 22A-DPPC, and 22A-DSPC sHDL to healthy Sprague Dawley rats. Based on cholesterol efflux from RAW 264.7 cells and LCAT-catalyzed esterification results *in vitro* we were expecting to see higher cholesterol mobilization and esterification for POPC and DMPC-based sHDL *in vivo*. However, the results of *in vivo* administration of 50 mg/kg of sHDL were reversed with 22A-DSPC showed significantly higher free cholesterol mobilization to the plasma compartment represented by the area under the effect curve (*AUEC*) $AUEC_{22A-DSPC}$ = 536.4 mg*h/dL compared to three other sHDL formulations with lower AUEC$_{22A-POPC}$ = 79.4 mg*h/dL, $AUEC_{22A-DMPC}$ = 126.5 mg*h/dL, and $AUEC_{22A-DPPC}$ = 215.0 mg*h/dL (**Fig. 5, Table 3**). Although the C_{max} of plasma EC was higher for DMPC-based sHDL, DSPC-based sHDL administration resulted in higher EC concentration at later time points and 3.5-fold greater *AUEC* values relative to DMPC-based sHDL (**Fig. 5D, Table 3**). The differences between *in vitro* and *in vivo* results could be attributed to differences in lipid

21

T_m affecting the *in vivo* circulation time. Our *in vivo* data supports this hypothesis where phospholipids with higher transition temperatures such as DSPC (T_m = 55°C) showed greater half-life and slower clearance than other phospholipids (**Fig. 5B**). Interestingly, the 22A peptide kinetics such as plasma half-life after administration of sHDL in rats did not follow phospholipid kinetics similar to the differences in PK parameters between lipid and peptide obtained with 22A- and 22A-P-sHDL. The half-life of 22A after 22A-DSPC infusion was nearly identical to 22A-DMPC, 22A-POPC, and 22A-DPPC formulations (3.3 h, 3.0 h, 3.3 h, and 3.3 h, respectively) (**Table 3**). Taken together, these results suggest that the ability of sHDL to mobilize cholesterol is strongly dependent on phospholipid composition and pharmacokinetics.

Remodeling of endogenous HDL in human plasma

To assess how different compositions of sHDL facilitate the remodeling of endogenous lipoproteins, all sHDL particles were incubated with human plasma for 1 hour at 1 mg/mL peptide concentration. The HDL sub-fractions were separated by size using 1D native PAGE electrophoresis and visualized by Western Blot using anti-ApoA-I antibody (**Fig. 6**). We have confirmed that anti-ApoA-I antibody does not recognize 22A, 21A or 22A-P, thus, we examined the impact of sHDL incubation on the remodeling of endogenous ApoA-I containing proteins. Compared to human plasma control incubated with PBS, incubation of plasma with 22A-sHDL, 21A-sHDL, and 22A-P-sHDL resulted in the remodeling of endogenous HDL indicated by a diminished signal for the large α-HDL and increased levels of lipid-poor ApoA-I. The effect of the phospholipid composition of sHDL on endogenous HDL remodeling was more prominent. Incubation of plasma with 22A-POPC resulted in a shift of HDL size from large α-HDL to smaller pre-β HDL. Incubation with 22A-DMPC showed the formation of even smaller pre-β HDL particles with a band of lipid-free ApoA-I. In contrast, plasma incubation with 22A-DSPC displayed very limited HDL remodeling, likely due to the rigidity of the DSPC lipid membrane and thus reduced

the insertion of endogenous ApoA-I. The 22A-DPPC incubation with plasma resulted in some reduction of α-HDL levels and formation of a predominant band of lipid-free ApoA-I. Overall, the extent of HDL remodeling was significantly affected by the phospholipid composition of sHDL. The sHDL prepared with high T_m phospholipids (22A-DPPC and 22A-DSPC) exhibited higher plasma stability and less remodeling.

Discussion

Our previous studies have shown that upon intravenous administration of sHDL, 22A peptide becomes rapidly hydrolyzed into 21A due to loss of terminal lysine (Tang *et al.*, 2017). The addition of C-terminal proline after the labile lysine in 22A afforded a resistant to proteolysis peptide as shown by incubation of 22A-P with rat plasma. The new peptide was successfully formulated into sHDL and dosed into rats. We expected to see longer circulation time and corresponding greater *in vivo* cholesterol mobilization for 22A-P-sHDL. As predicted *in vitro*, the half-life of 22A-P in animals was extended from 2.1 to 4.2 hours and AUC for 22A-P is nearly 3-fold higher. However, the longer circulation time of 22A-P *in vivo* did not translate into a higher cholesterol mobilization profile by 22A-P-sHDL compared to 22A-sHDL. Furthermore, the AUC of the phospholipid component of 22A-P-sHDL and 22A-sHDL were also not affected by the extension of the peptide half-life. When sHDL particles prepared with the same peptide 22A and different phospholipids (POPC, DMPC, DPPC, or DSPC) were administered to rats the peptide half-life was similar for all four formulations (3.2 ± 0.1 h). However, the phospholipid half-life varied dramatically with DSPC circulating for 6.0 h compared to 1.0 - 3.3 h for other lipids. The trend of phospholipid circulation time for each sHDL formulation in animal serum was similar to that of cholesterol mobilization (22A-DSPC> 22A-DPPC, 22A-DMPC> 22A-POPC). Moreover, these findings are further supported by our HDL remodeling results, showing only limited interaction of 22A-DSPC with endogenous HDL, which could extend circulation half-life. The limited interaction between sHDL and endogenous lipoproteins is likely due to the difficulty of protein insertion in the gel membrane of DSPC (T_m of 55 °C, above physiological temperature) as was observed *in vitro* for 22A-DSPC interaction with LCAT. Altogether, the data suggest that the pharmacokinetics of peptide and lipid components in sHDL are not interdependent and original infused sHDL particles may dissociate or become remodeled upon administration *in vivo*. In addition, the phospholipid rather than peptide component in sHDL has a major impact on the ability to mobilize cholesterol *in vivo*. However, it is important to note that the peptide sequence modifications performed by us

were rather minor. It has been shown that different sequences of ApoA-I mimetic peptides have measurable differences in cholesterol efflux *in vitro* and variable *in vivo* performance (Sethi *et al.*, 2008; Wool *et al.*, 2008; Amar *et al.*, 2010; Bielicki *et al.*, 2010).

Several other groups reported on the discordance between the PK of protein and phospholipid components of HDL *in vivo*. Xu *et al.* investigated the fate of ApoA-I protein and phospholipid after *in vivo* administration of HDL in an attempt to interrogate the validity of the reverse cholesterol transport pathway (Xu *et al.*, 2017). The investigators used ABCA1-derived ApoA-I-HDL with radiolabeled components and reported that phospholipids and ApoA-I enter different pathways for clearance in mice. The authors suggested that after the administration of radiolabeled ApoA-I-HDL, phospholipids were rapidly cleared by the liver and also transferred to LDL while ApoA-I fused with endogenous HDL and circulated longer. CSL-112, the ApoA-I-soybean phosphatidylcholine sHDL product undergoing phase III clinical trial, is believed to undergo remodeling in human plasma with the generation of lipid-poor ApoA-I that is important for cholesterol efflux (Didichenko *et al.*, 2016). Another sHDL product in clinical development, CER-001, composed from ApoA-I and primarily sphingomyelin, have shown differences, specifically longer half-life for phospholipid (~46 h) relatively to ApoA-I (~10 h) (Keyserling *et al.*, 2011; Tardy *et al.*, 2014). We also found that incorporation of polyethylene glycol-modified lipids in ApoA-I peptide-based sHDL extended circulation time for lipids and prolonged the duration of mobilized cholesterol circulation but had not altered ApoA-I peptide PK (Li *et al.*, 2018). Therefore, peptide and lipid components of sHDL may both contribute to cholesterol mobilization, however not as intact nanoparticles, but rather as separate entities via different mechanisms.

The phospholipid composition also impacted the ease of sHDL preparation, purity, and size of the resulting nanoparticles and their stability *in vitro* and *in vivo*. The sHDL prepared with DSPC, DPPC, and DMPC showed relatively similar narrow size distributions and high purities while sHDL prepared with POPC appeared to be more heterogeneous with larger average particle sizes and a presence of liposomal impurities. This relative difficulty of forming pure POPC-based

sHDL particles has been reported previously and was attributed to the fluidity and instability of the POPC membrane at room temperature, which was well above the phospholipid's T_m (Patel *et al.*, 2019). The sHDL prepared with saturated lipids appeared to be more homogeneous and pure but required heating particles above lipid T_m during preparation to facilitate ApoA-I peptide-lipid binding. In addition, the presence of unsaturated double bonds in lipids such as POPC could result in phospholipid oxidation, although this phenomenon was not investigated in this study.

Interestingly, we also observed a discordance between *in vitro* and *in vivo* results for sHDL prepared with different phospholipids and peptides. The *in vitro* trends for higher cholesterol efflux and superior ability to activate LCAT for 22A-POPC and 22A-DMPC did not translate into higher cholesterol mobilization and esterification *in vivo*. The free cholesterol mobilization and circulation time appear to be closely following the circulation time of phospholipids, with the longer circulating saturated DSPC exhibiting higher C_{max} for FC mobilization and $AUEC$. Thus, the ease of cholesterol incorporation in unsaturated 22A-POPC becomes of limited significance *in vivo* due to rapid elimination of POPC. The esterification seems to follow the same trend, as faster LCAT-catalyzed lipolysis and sterol esterification did not translate to greater C_{max} and $AUEC$ for EC *in vivo*. However, it is important to point out that the actual rate of EC formation and LCAT activation *in vivo* was not directly measured in this study and will require additional experiments as described by Turner *et a*l. (Turner *et al.*, 2012). The stability of 22A-P is greatly improved *in vivo* relative to 22A, however phospholipid PK appeared to be unchanged and cholesterol mobilization follows phospholipid PK. One of the explanations for this may be that both 22A and 22A-P are capable of forming sHDL *in vitro* and maintaining sHDL stability *in vivo*, as the structures of all three peptides used by us are very similar. It is also important to point out that other groups had seen discordance between showing some structure-activity relationship for ApoA-I peptides *in vitro* and seeing no statistical differences in their pharmacological effects *in vivo* (Ditiatkovski *et al.*, 2017).

Our data support the complexity of RCT and highlights that both ApoA-I protein/peptide and lipid components of sHDL contribute to the RCT pathway. The study also highlights that the

phospholipid composition of sHDL is the driving force for cholesterol mobilization *in vivo* and we

plan to further examine if higher cholesterol mobilization for sHDL composed of saturated lipids

will lead to greater anti-atherosclerosis effect in a murine model of the disease.

Acknowledgments

Authorship Contributions

Participated in research design: Fawaz, Kim, Schwendeman, Tesmer

Conducted experiments: Fawaz, Kim, Ming, Xia, Ackerman, Olsen, Pogozheva

Performed data analysis: Fawaz, Kim, Li, Schwendeman

Wrote and contributed to the writing of the manuscript: Fawaz, Kim, Pogozheva, Schwendeman, Tesmer

References

Amar MJA, D'Souza W, Turner S, Demosky S, Sviridov Denis, Stonik J, Luchoomun J, Voogt J, Hellerstein M, Sviridov Dmitri, and Remaley AT (2010) 5A apolipoprotein mimetic peptide promotes cholesterol efflux and reduces atherosclerosis in mice. *J Pharmacol Exp Ther* **334**:634–41.

Anantharamaiah GM, Venkatachalapathi Y V, Brouillette CG, and Segrest JP (1990) Use of synthetic peptide analogues to localize lecithin:cholesterol acyltransferase activating domain in apolipoprotein A-I. *Arterioscler An Off J Am Hear Assoc Inc* **10**:95–105.

Andrews J, Janssan A, Nguyen T, Pisaniello AD, Scherer DJ, Kastelein JJP, Merkely B, Nissen SE, Ray K, Schwartz GG, Worthley SG, Keyserling C, Dasseux J-L, Butters J, Girardi J, Miller R, and Nicholls SJ (2017) Effect of serial infusions of reconstituted high-density lipoprotein (CER-001) on coronary atherosclerosis: rationale and design of the CARAT study. *Cardiovasc Diagn Ther* **7**:45–51.

Assmann G, Schmitz G, Donath N, and Lekim D (1978) Phosphatidylcholine Substrate Specificity of Lecithin: Cholesterol Acyltransferase. *Scand J Clin Lab Invest* **38**:16–20.

Asztalos BF, Schaefer EJ, Horvath K V, Yamashita S, Miller M, Franceschini G, and Calabresi L (2007) Role of LCAT in HDL remodeling: investigation of LCAT deficiency states. *J Lipid Res* **48**:592–9.

Bielicki JK, Zhang H, Cortez Y, Zheng Y, Narayanaswami V, Patel A, Johansson J, and Azhar S (2010) A new HDL mimetic peptide that stimulates cellular cholesterol efflux with high efficiency greatly reduces atherosclerosis in mice. *J Lipid Res* **51**:1496–503.

Bolin DJ, and Jonas A (1996) Sphingomyelin inhibits the lecithin-cholesterol acyltransferase reaction with reconstituted high density lipoproteins by decreasing enzyme binding. *J Biol Chem* **271**:19152–8.

Dasseux J-L, Sekul R, Buttner K, Cornut I, Metz G, and Dufourcq J (1999) Apolipoprotein AI agonists and their use to treat dyslipidemic disorders.

Dasseux J, Sekul R, Büttner K, Cornut I, Metz G, and Dufourcq J (2004) Multimeric Apoa-I agonist compounds.

Datta G, Chaddha M, Hama S, Navab M, Fogelman AM, Garber DW, Mishra VK, Epand RM, Epand RF, Lund-Katz S, Phillips MC, Segrest JP, and Anantharamaiah GM (2001) Effects of increasing hydrophobicity on the physical-chemical and biological properties of a class A amphipathic helical peptide. *J Lipid Res* **42**:1096–104.

Davidson WS, Gillotte KL, Lund-Katz S, Johnson WJ, Rothblat GH, and Phillips MC (1995) The effect of high density lipoprotein phospholipid acyl chain composition on the efflux of cellular free cholesterol. *J Biol Chem* **270**:5882–90.

Di Bartolo BA, Nicholls SJ, Bao S, Rye K-A, Heather AK, Barter PJ, and Bursill C (2011) The apolipoprotein A-I mimetic peptide ETC-642 exhibits anti-inflammatory properties that are comparable to high density lipoproteins. *Atherosclerosis* **217**:395–400.

Didichenko SA, Navdaev A V., Cukier AMO, Gille A, Schuetz P, Spycher MO, Thérond P, Chapman MJ, Kontush A, and Wright SD (2016) Enhanced HDL Functionality in Small HDL Species Produced Upon Remodeling of HDL by Reconstituted HDL, CSL112. *Circ Res* **119**:751–763.

Ditiatkovski M, Palsson J, Chin-Dusting J, Remaley AT, and Sviridov D (2017) Apolipoprotein A-I Mimetic Peptides: Discordance Between In Vitro and In Vivo Properties-Brief Report. *Arterioscler Thromb Vasc Biol* **37**:1301–1306.

Duffy D (2018) Identifier: NCT03473223, Study to Investigate CSL112 in Subjects With Acute Coronary Syndrome (AEGIS-II); March 21, 2018.

Homan R, Esmaeil N, Mendelsohn L, and Kato GJ (2013) A fluorescence method to detect and quantitate sterol esterification by lecithin:cholesterol acyltransferase. *Anal Biochem* **441**:80–86.

Keyserling CH, Hunt TL, Klepp HM, Scott RA, Barbaras R, Schwendeman A, Lalwani N, and Dasseux J-L (2011) Abstract 15525: CER-001, a Synthetic HDL-Mimetic, Safely Mobilizes

Cholesterol in Healthy Dyslipidemic Volunteers. *Circulation* **124**.

Khan M, Drake S, Crockatt J, and Dasseux J (2003) Single-dose intravenous infusion of ETC-642, a 22-Mer ApoA-I analogue and phospholipids complex, elevates HDL-C in atherosclerosis patients. *Circulation* **108**:563–564.

Krieger M (1999) Charting the fate of the "good cholesterol": identification and characterization of the high-density lipoprotein receptor SR-BI. *Annu Rev Biochem* **68**:523–58.

Li D, Fawaz M V., Morin EE, Ming R, Sviridov D, Tang J, Ackermann R, Olsen K, Remaley AT, and Schwendeman A (2018) Effect of Synthetic High Density Lipoproteins Modification with Polyethylene Glycol on Pharmacokinetics and Pharmacodynamics. *Mol Pharm* **15**:83–96.

Li D, Gordon S, Schwendeman A, and Remaley AT (2015) Apolipoprotein Mimetic Peptides for Stimulating Cholesterol Efflux, in *Apolipoprotein Mimetics in the Management of Human Disease* pp 29–42.

Lomize AL, Lomize MA, Krolicki SR, and Pogozheva ID (2017) Membranome: a database for proteome-wide analysis of single-pass membrane proteins. *Nucleic Acids Res* **45**:D250–D255.

Lomize MA, Pogozheva ID, Joo H, Mosberg HI, and Lomize AL (2012) OPM database and PPM web server: resources for positioning of proteins in membranes. *Nucleic Acids Res* **40**:D370–D376.

Miles J, Khan M, Painchaud C, Lalwani N, Drake S, and Dasseux J (2004) P105 Single-dose Tolerability, Pharmacokinetics, and Cholesterol Mobilization in Hdl-c Fraction Following Intravenous Administration of Etc-642, a 22-mer Apoa-i Analogue and Phospholipids Complex, in Atherosclerosis Patients. *Arterioscler Thromb Vasc Biol J Am Hear Assoc* **24**:e-19.

Navab M, Anantharamaiah G, Reddy ST, and Fogelman AM (2006) Apolipoprotein A-I mimetic peptides and their role in atherosclerosis prevention. *Nat Clin Pract Cardiovasc Med*

3:540–547.

Navab M, Anantharamaiah GM, Hama S, Hough G, Reddy ST, Frank JS, Garber DW, Handattu

S, and Fogelman AM (2005) D-4F and Statins Synergize to Render HDL Antiinflammatory

in Mice and Monkeys and Cause Lesion Regression in Old Apolipoprotein E–Null Mice.

Arterioscler Thromb Vasc Biol **25**:1426–1432.

Navab M, Anantharamaiah GMM, Reddy ST, Hama S, Hough G, Grijalva VR, Yu N, Ansell BJ,

Datta G, Garber DW, and Fogelman AM (2005) Apolipoprotein A-I mimetic peptides.

Arterioscler Thromb Vasc Biol **25**:1325–31.

Nicholls SJ, Andrews J, Kastelein JJP, Merkely B, Nissen SE, Ray KK, Schwartz GG, Worthley

SG, Keyserling C, Dasseux J-L, Griffith L, Kim SW, Janssan A, Di Giovanni G, Pisaniello

AD, Scherer DJ, Psaltis PJ, and Butters J (2018) Effect of Serial Infusions of CER-001, a

Pre-β High-Density Lipoprotein Mimetic, on Coronary Atherosclerosis in Patients Following

Acute Coronary Syndromes in the CER-001 Atherosclerosis Regression Acute Coronary

Syndrome Trial. *JAMA Cardiol* **3**:815.

Nissen SE, Tsunoda T, Tuzcu EM, Schoenhagen P, Cooper CJ, Yasin M, Eaton GM, Lauer MA,

Sheldon WS, Grines CL, Halpern S, Crowe T, Blankenship JC, Kerensky R, SE N, WJ C,

CM B, V G, CR S, PK S, SE N, M S, HJ E, G M, P S, BG B, G F, B P, JW J, RP B, GG S,

EJ T, T T, and JC F (2003) Effect of Recombinant ApoA-I Milano on Coronary

Atherosclerosis in Patients With Acute Coronary Syndromes. *JAMA* **290**:2292.

Ohvo-Rekilä H, Ramstedt B, Leppimäki P, and Peter Slotte J (2002) Cholesterol interactions

with phospholipids in membranes. *Prog Lipid Res* **41**:66–97.

Parks JS, and Gebre AK (1997) Long-chain polyunsaturated fatty acids in the sn-2 position of

phosphatidylcholine decrease the stability of recombinant high density lipoprotein

apolipoprotein A-I and the activation energy of the lecithin:cholesterol acyltransferase

reaction. *J Lipid Res* **38**:266–75.

Patel H, Ding B, Ernst K, Shen L, Yuan W, Tang J, Drake LR, Kang J, Li Y, Chen Z, and

Schwendeman A (2019) Characterization of apolipoprotein A-I peptide phospholipid

interaction and its effect on HDL nanodisc assembly. *Int J Nanomedicine* **14**:3069–3086.

Ramstedt B, and Slotte JP (1999) Interaction of cholesterol with sphingomyelins and acyl-chain-

matched phosphatidylcholines: a comparative study of the effect of the chain length.

Biophys J **76**:908–15.

Reißer S, Strandberg E, Steinbrecher T, and Ulrich AS (2014) 3D Hydrophobic Moment Vectors

as a Tool to Characterize the Surface Polarity of Amphiphilic Peptides. *Biophys J*

106:2385–2394.

Remaley AT, Stonik JA, Demosky SJ, Neufeld EB, Bocharov A V., Vishnyakova TG, Eggerman

TL, Patterson AP, Duverger NJ, Santamarina-Fojo S, and Brewer HB (2001)

Apolipoprotein Specificity for Lipid Efflux by the Human ABCAI Transporter. *Biochem

Biophys Res Commun* **280**:818–823.

Remaley AT, Thomas F, Stonik JA, Demosky SJ, Bark SE, Neufeld EB, Bocharov A V,

Vishnyakova TG, Patterson AP, Eggerman TL, Santamarina-Fojo S, and Brewer HB (2003)

Synthetic amphipathic helical peptides promote lipid efflux from cells by an ABCA1-

dependent and an ABCA1-independent pathway. *J Lipid Res* **44**:828–36.

Schwendeman A, Sviridov DO, Yuan W, Guo Y, Morin EE, Yuan Y, Stonik J, Freeman L, Ossoli

A, Thacker S, Killion S, Pryor M, Chen YE, Turner S, and Remaley AT (2015) The effect of

phospholipid composition of reconstituted HDL on its cholesterol efflux and anti-

inflammatory properties. *J Lipid Res* **56**:1727–37.

Sethi AA, Stonik JA, Thomas F, Demosky SJ, Amar M, Neufeld E, Brewer HB, Davidson WS,

Souza W D', Sviridov D, Remaley AT, D'Souza W, Sviridov D, and Remaley AT (2008)

Asymmetry in the lipid affinity of bihelical amphipathic peptides. A structural determinant for

the specificity of ABCA1-dependent cholesterol efflux by peptides. *J Biol Chem*

283:32273–82.

Small D. (1986) *Handbook of lipid research. The Physical Chemistry*.

33

Sorci-Thomas M, Kearns MW, and Lee JP (1993) Apolipoprotein A-I domains involved in lecithin-cholesterol acyltransferase activation. Structure:function relationships. *J Biol Chem* **268**:21403–9.

Soutar AK, Garner CW, Baker HN, Sparrow JT, Jackson RL, Gotto AM, and Smith LC (1975) Effect of the human plasma apolipoproteins and phosphatidylcholine acyl donor on the activity of lecithin: cholesterol acyltransferase. *Biochemistry* **14**:3057–64.

Sparks DL, Frank PG, and Neville TA (1998) Effect of the surface lipid composition of reconstituted LPA-I on apolipoprotein A-I structure and lecithin: cholesterol acyltransferase activity. *Biochim Biophys Acta* **1390**:160–72.

Sreerama N, and Woody RW (2000) Estimation of Protein Secondary Structure from Circular Dichroism Spectra: Comparison of CONTIN, SELCON, and CDSSTR Methods with an Expanded Reference Set. *Anal Biochem* **287**:252–260.

Subbaiah P V, Liu M, Bolan PJ, and Paltauf F (1992) Altered positional specificity of human plasma lecithin-cholesterol acyltransferase in the presence of sn-2 arachidonoyl phosphatidyl cholines. Mechanism of formation of saturated cholesteryl esters. *Biochim Biophys Acta* **1128**:83–92.

Tang J, Li D, Drake L, Yuan W, Deschaine S, Morin EE, Ackermann R, Olsen K, Smith DE, and Schwendeman A (2017) Influence of route of administration and lipidation of apolipoprotein A-I peptide on pharmacokinetics and cholesterol mobilization. *J Lipid Res* **58**:124–136.

Tardif J-C, Grégoire J, L'Allier PL, Ibrahim R, Lespérance J, Heinonen TM, Kouz S, Berry C, Basser R, Lavoie M-A, Guertin M-C, and Rodés-Cabau J (2007) Effects of reconstituted high-density lipoprotein infusions on coronary atherosclerosis: a randomized controlled trial. *JAMA* **297**:1675–82.

Tardy C, Goffinet M, Boubekeur N, Ackermann R, Sy G, Bluteau A, Cholez G, Keyserling C, Lalwani N, Paolini JF, Dasseux J-L, Barbaras R, and Baron R (2014) CER-001, a HDL-mimetic, stimulates the reverse lipid transport and atherosclerosis regression in high

cholesterol diet-fed LDL-receptor deficient mice. *Atherosclerosis* **232**:110–118.

Tricoci P, D'Andrea DM, Gurbel PA, Yao Z, Cuchel M, Winston B, Schott R, Weiss R, Blazing
MA, Cannon L, Bailey A, Angiolillo DJ, Gille A, Shear CL, Wright SD, and Alexander JH
(2015) Infusion of Reconstituted High-Density Lipoprotein, CSL112, in Patients With
Atherosclerosis: Safety and Pharmacokinetic Results From a Phase 2a Randomized
Clinical Trial. *J Am Heart Assoc* **4**:e002171.

Turner S, Voogt J, Davidson M, Glass A, Killion S, Decaris J, Mohammed H, Minehira K, Boban
D, Murphy E, Luchoomun J, Awada M, Neese R, and Hellerstein M (2012) Measurement of
Reverse Cholesterol Transport Pathways in Humans: In Vivo Rates of Free Cholesterol
Efflux, Esterification, and Excretion. *J Am Heart Assoc* **1**:e001826.

Vecoli C, Cao J, Neglia D, Inoue K, Sodhi K, Vanella L, Gabrielson KK, Bedja D, Paolocci N,
L'Abbate A, and Abraham NG (2011) Apolipoprotein A-I mimetic peptide L-4F prevents
myocardial and coronary dysfunction in diabetic mice. *J Cell Biochem* **112**:2616–2626.

Wang N, Lan D, Chen W, Matsuura F, and Tall AR (2004) ATP-binding cassette transporters
G1 and G4 mediate cellular cholesterol efflux to high-density lipoproteins. *Proc Natl Acad
Sci* **101**:9774–9779.

Wool GD, Reardon CA, and Getz GS (2008) Apolipoprotein A-I mimetic peptide helix number
and helix linker influence potentially anti-atherogenic properties. *J Lipid Res* **49**:1268–83.

Xu B, Gillard BK, Gotto AM, Rosales C, and Pownall HJ (2017) ABCA1-Derived Nascent High-
Density Lipoprotein–Apolipoprotein AI and Lipids Metabolically Segregate. *Arterioscler
Thromb Vasc Biol* **37**:2260–2270.

Footnotes

Legends for Figures

Figure 1. Size distribution and purity of sHDL prepared with various peptide (A, B) and phospholipid (C, D) compositions. The size was determined by dynamic light scattering (DLS) (A, C) and purity was determined by gel permeation chromatography (GPC) (B, D).

Figure 2. Effect of peptides and sHDL on cholesterol efflux. Free peptides (22A , 21A, 22A-P) were used to efflux cholesterol from BHK cells stably transfected with ABCA1 transporter (A) and sHDL (22A-DMPC, 21A-DMPC, 22A-P-DMPC and 22A-POPC, 22A-DMPC, 22A-DPPC, 22A-DSPC) were utilized to efflux cholesterol from RAW 264.7 macrophage cells (B, C) at 0.01, 0.03, and 0.1 mg/mL for 18 hrs. The contribution of ABCA1 transporter was determined by subtracting efflux values of Mock-transfected cell line from ABCA1-transfected cell line (n=3, mean $\pm$ SEM). Statistical differences were compared to 22A peptide or 22A-DMPC with one-way ANOVA analysis with Dunnett's post-hoc test. $P < 0.05$ was considered statistically significant $^{*}P < 0.05$, $^{**}P < 0.01$, $^{***}P < 0.001$

Figure 3. Effect of peptide and phospholipid composition in sHDL on LCAT lipolysis and esterification rates. (A, B) The rate of sHDL lipolysis was determined by incubating sHDL (0.1 mg/mL) prepared with variable peptide composition (22A-DMPC, 21A-DMPC, 22A-P-DMPC) or variable phospholipid composition (22A-POPC, 22A-DMPC, 22A-DPPC, 22A-DSPC) with human rhLCAT (15 μg/mL) at 37 $°$C for 0, 5, 15, 30, 60, 90, and 120 min. The concentration of phospholipid at each time point was determined by LC-MS and the rate of lipolysis calculated from the slope of the concentration of the starting material versus time. LCAT esterification activity was measured for sHDL containing fluorescent cholesterol analog, dehydroergosterol (DHE) (C, D). The initial reaction rates (V_0) are plotted as a function of DHE concentration and the data were

37

fitted into the Michaelis-Menten kinetic equation to calculate V_{max} and Km (n=3, mean ± SEM). Statistical differences were compared to 22A peptide or 22A-DMPC with one-way ANOVA analysis with Dunnett's post-hoc test. $P < 0.05$ was considered statistically significant $^{*}P < 0.05$, $^{**}P < 0.01$, $^{***}P < 0.001$

Figure 4. Pharmacokinetic analysis of 22A and 22A-P peptides (A) or total phospholipids (B) in rat serum. Pharmacodynamic assessment of free cholesterol (C) and esterified cholesterol (D) mobilization in rat serum. Healthy male Sprague-Dawley rats were given a single tail vein injection of 50 mg/kg (based on peptide) of 22A-POPC-DPPC or 22A-P-POPC-DPPC and blood samples were collected at pre-dose and 0.25, 0.5, 1, 2, 4, 8, and 24 h after sHDL administration. Serum concentrations of peptides were determined by LC-MS while concentrations of phospholipids, free cholesterol, and esterified cholesterol were measured enzymatically (n=3). Statistical difference was compared with two-tailed Student's t-test. $P < 0.05$ was considered statistically significant $^{*}P < 0.05$, $^{**}P < 0.01$, $^{***}P < 0.001$

Figure 5. Pharmacokinetic analysis of 22A (A) and total phospholipids (B) in rat serum. Pharmacodynamic assessment of free cholesterol (C) and esterified cholesterol (D) mobilization in rat serum. Healthy male Sprague-Dawley rats were given a single tail vein injection of 50 mg/kg (based on peptide) of 22A-POPC, 22A-DMPC, 22A-DPPC, or 22A-DSPC and blood samples were collected at pre-dose and 0.25, 0.5, 1, 2, 4, 8, and 24 h after sHDL administration. Serum concentrations of peptides were determined by LC-MS while concentrations of phospholipids, free cholesterol, and esterified cholesterol were measured enzymatically (n=3). Statistical differences for 22A-phospholipid were compared to 22A-DMPC with one-way ANOVA analysis with Dunnett's post-hoc test. $P < 0.05$ was considered statistically significant. $P < 0.05$, $^{**}P < 0.01$, $^{***}P < 0.001$

Figure 6. Effect of sHDL incubation with human plasma on endogenous HDL remodeling. Various compositions of sHDL were incubated in human plasma at 1 mg/mL for 1 h at 37°C. Lipoproteins were separated by 1-D native page electrophoresis and visualized by western blot using anti-apoA-I antibody.
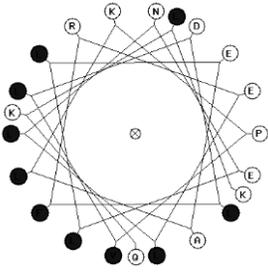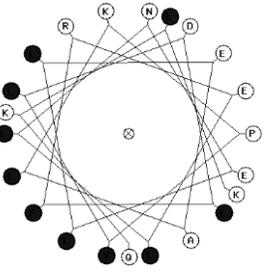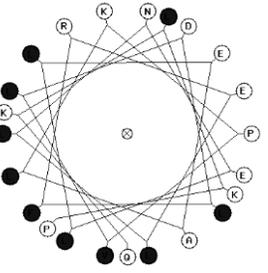
Tables

Peptide name	22A	21A	22A-P
Sequence	PVLDLFRELLNELLEALK QKLK	PVLDLFRELLNELLEAL KQKL	PVLDLFRELLNELLEAL KQKLKP
Helical wheel plot[a]			
Hydrophobic moment vector (A*kT/e)[b]	11.1	10.0	9.9
ΔG_{hel} (kcal/mol)[c]	-19.8	-19.4	-19.8
ΔG_{tran} (kcal/mol)[c]	-14.7	-13.4	-14.7
D (Å)[c]	11.8 ± 3.6	8.1 ± 4.6	11.8 ± 3.6
Helical content of lipid-free peptide (%)[d]	76.6	79.0	76.5
Helical content of lipid-bound peptide (%)[d]	93.9	90.9	81.6
Peptide plasma stability (%)[e]	48.4 ± 10.6	96.8 ± 5.4	89.3 ± 12.5

Table 1. Biophysical characterization of peptides. [a]Helical wheel plots were generated using the online tool called Helixator where hydrophobic amino acids were highlighted in blue. [b]Hydrophobic moments were calculated by the 3D Hydrophobic Moment Vector Calculator. [c]Helix stability (ΔG_{hel}), transfer energy from water to membrane (ΔG_{tran}), and tilt angle in membranes were predicted by FMAP server for 22A, 21A, and 22A-P peptide sequences; [d]Helical content of lipid-free and lipid-bound peptides was determined by circular dichroism; [e]Peptide stability in rat plasma was determined by LC-MS shown as percent remaining peptide following 24 h incubation at 37°C (n=3, mean ± standard deviation).

	Parameters	Groups	
		22A-sHDL	22A-P-sHDL
Peptide	AUC (mg*h/dL)	554.0 (22.0)	1721.0 (10.6)[***]
	K (h^{-1})	0.3 (25.8)	0.2 (12.0)
	$T_{1/2}$ (h)	2.1 (22.4)	4.2 (10.8)[**]
	CL (dL/h)	2.3 (21.8)	0.7 (10.9)[**]
	V_d (dL)	6.9 (7.7)	4.4 (6.2)[**]
PL	AUC (mg*h/dL)	424.4 (15.7)	371.8 (23.5)
	K (h^{-1})	0.4 (23.8)	0.5 (16.0)
	$T_{1/2}$ (h)	1.8 (18.8)	1.3 (11.4)[*]
	CL (dL/h)	0.1 (7.7)	0.1 (7.0)
	V_d (dL)	0.1 (21.4)	0.1 (2.1)
FC	$T_{max,E}$ (h)	0.5 (0.0)	0.8 (33.3)
	E_{max} (mg/dL)	46.7 (5.8)	44.4 (13.0)
	$AUEC$ (mg*h/dL)	158.0 (19.1)	175.3 (28.5)
EC	$T_{max,E}$ (h)	0.42 (24.5)	0.4 (33.3)
	E_{max} (mg/dL)	51.3 (31.8)	42.2 (37.3)
	$AUEC$ (mg*h/dL)	166.8 (12.8)	164.4 (31.8)

Table 2. Pharmacokinetic and pharmacodynamic parameters (%CV) of peptide, total phospholipids (PL), free cholesterol (FC), and esterified cholesterol (EC) after 50 mg/kg doses of 22A-sHDL and 22A-P-sHDL treatments. Data were shown as mean with CV%. [*]$P<0.05$, [**]$P < 0.01$, [***]$P < 0.001$. AUC: the area under the curve. K: elimination rate constant. $T_{1/2}$: the half-life of elimination. CL: total clearance. V_d: volume of distribution. $T_{max,E}$: time at which the E_{max} is observed. E_{max}: the maximum plasma concentration of different cholesterol species. $AUEC$: the area under the effect curve.

	Parameters	Groups			
		22A-POPC	22A-DMPC	22A-DPPC	22A-DSPC
Peptide	AUC (mg*h/dL)	364.0 (8.6)**	662.0 (10.0)	464.3 (15.2)*	687.2 (17.7)
	K (h⁻¹)	0.2 (6.0)	0.2 (1.7)	0.2 (2.4)	0.2 (4.0)
	T ½ (h)	3.3 (6.2)	3.0 (1.8)	3.3 (2.4)	3.3 (4.2)
	CL (dL/h)	5.6 (11.8)**	3.2 (13.9)	4.6 (17.4)	2.9 (25.2)
	V_d (dL)	27.1 (16.7)**	14.0 (15.5)	21.9 (19.0)	13.7 (29.1)
PL	AUC (mg*h/dL)	371.6 (29.0)	703.2 (23.2)	934.9 (22.8)	2396 (21.1)***
	K (h⁻¹)	0.7 (10.6)***	0.2 (4.4)	0.3 (16.8)	0.0 (12.6)**
	T ½ (h)	1.0 (9.8)***	3.3 (4.4)	2.2 (18.6)*	6.0 (12.4)***
	CL (dL/h)	0.1 (22.2)	0.1 (23.3)	0.0 (27.7)***	0.0 (27.3)***
	V_d (dL)	0.2 (29.8)	0.3 (23.3)	0.2 (45.9)	0.1 (16.0)*
FC	$T_{max,E}$ (h)	0.7 (35.4)	0.4 (28.3)	0.7 (35.4)	1.3 (35.4)*
	E_{max} (mg/dL)	25.8 (36.8)	37.6 (19.8)	44.8 (5.1)	51.5 (15.3)
	AUEC (mg*h/dL)	79.4 (33.9)	126.5 (10.0)	215.0 (20.9)	536.4 (19.1)***
EC	$T_{max,E}$ (h)	0.5 (70.7)	0.8 (28.3)	0.9 (84.3)	6.7 (28.3)**
	E_{max} (mg/dL)	7.7 (65.2)	28.2 (30.3)	24.9 (13.7)	20.6 (24.7)
	AUEC (mg*h/dL)	84.8 (65.3)	93.3 (41.9)	98.9 (31.6)	334.7 (18.0)**

Table 3. Pharmacokinetic and pharmacodynamic parameters (%CV) of 22A peptide, total phospholipids (PL), free cholesterol (FC), and esterified cholesterol (EC) after 50 mg/kg doses of 22A-POPC, 22A-DMPC, 22A-DPPC, and 22A-DSPC sHDL treatments. Data were shown as mean with CV%. *P<0.05, **P < 0.01, ***P < 0.001. *AUC*: the area under the curve. *K*: elimination rate constant. $T_{1/2}$: the half-life of elimination. *CL*: total clearance. V_d: volume of distribution. $T_{max,E}$: time at which the E_{max} is observed. E_{max}: the maximum plasma concentration of different cholesterol species. *AUEC*: the area under the effect curve.
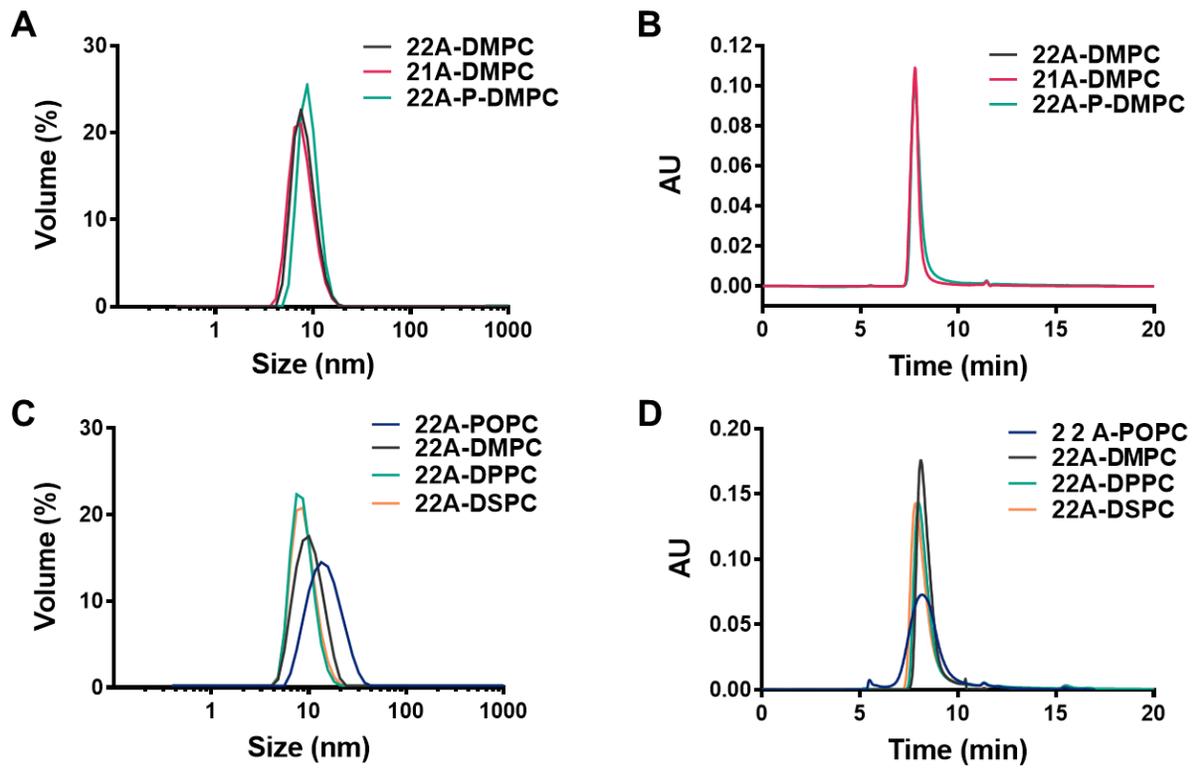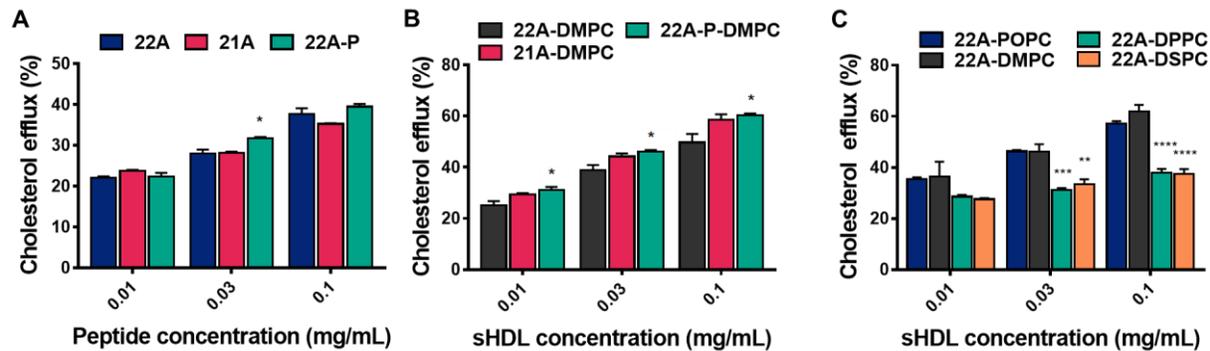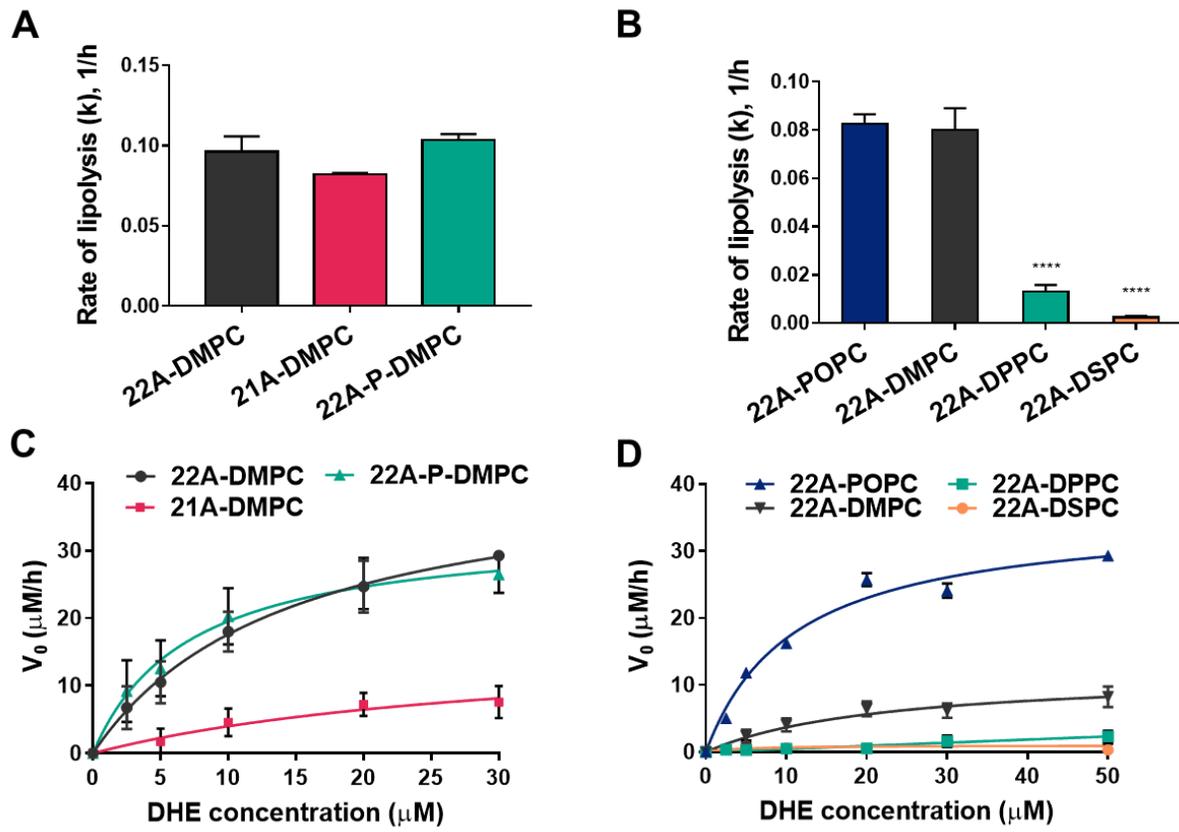
Figure 1

43

Figure 2

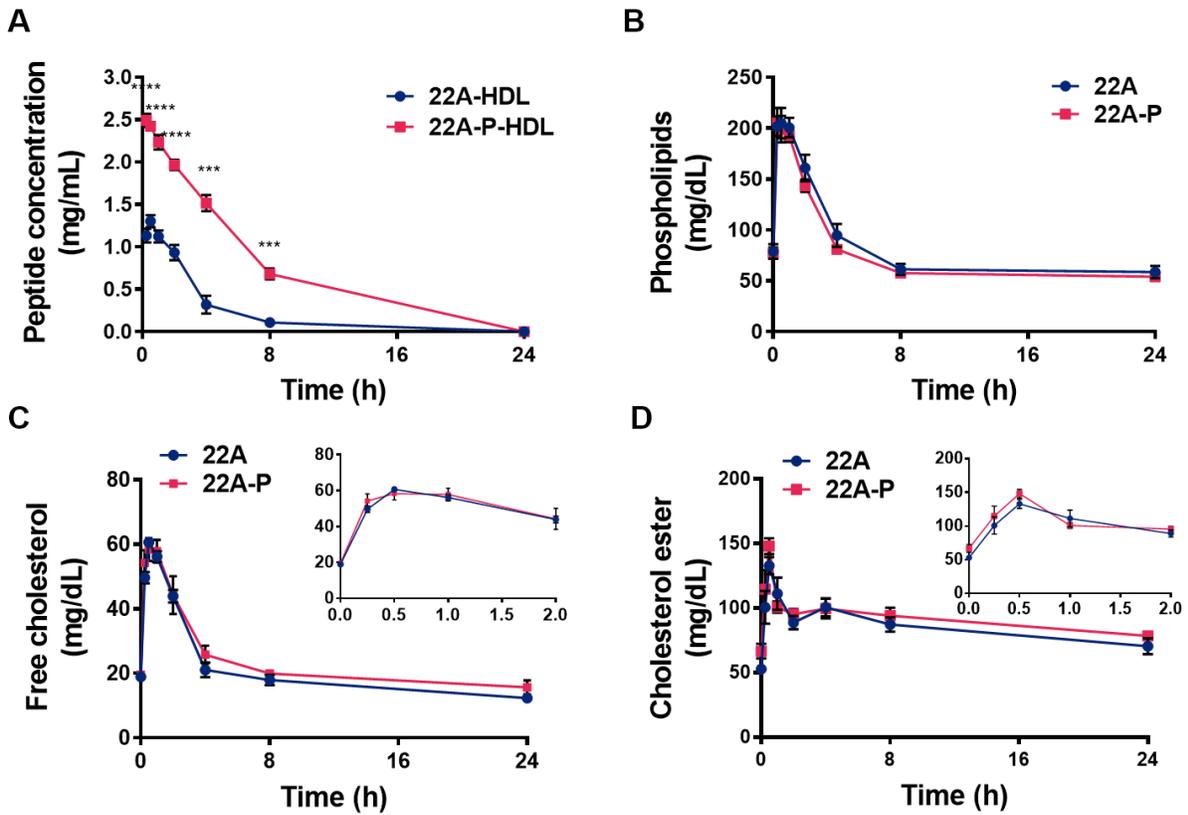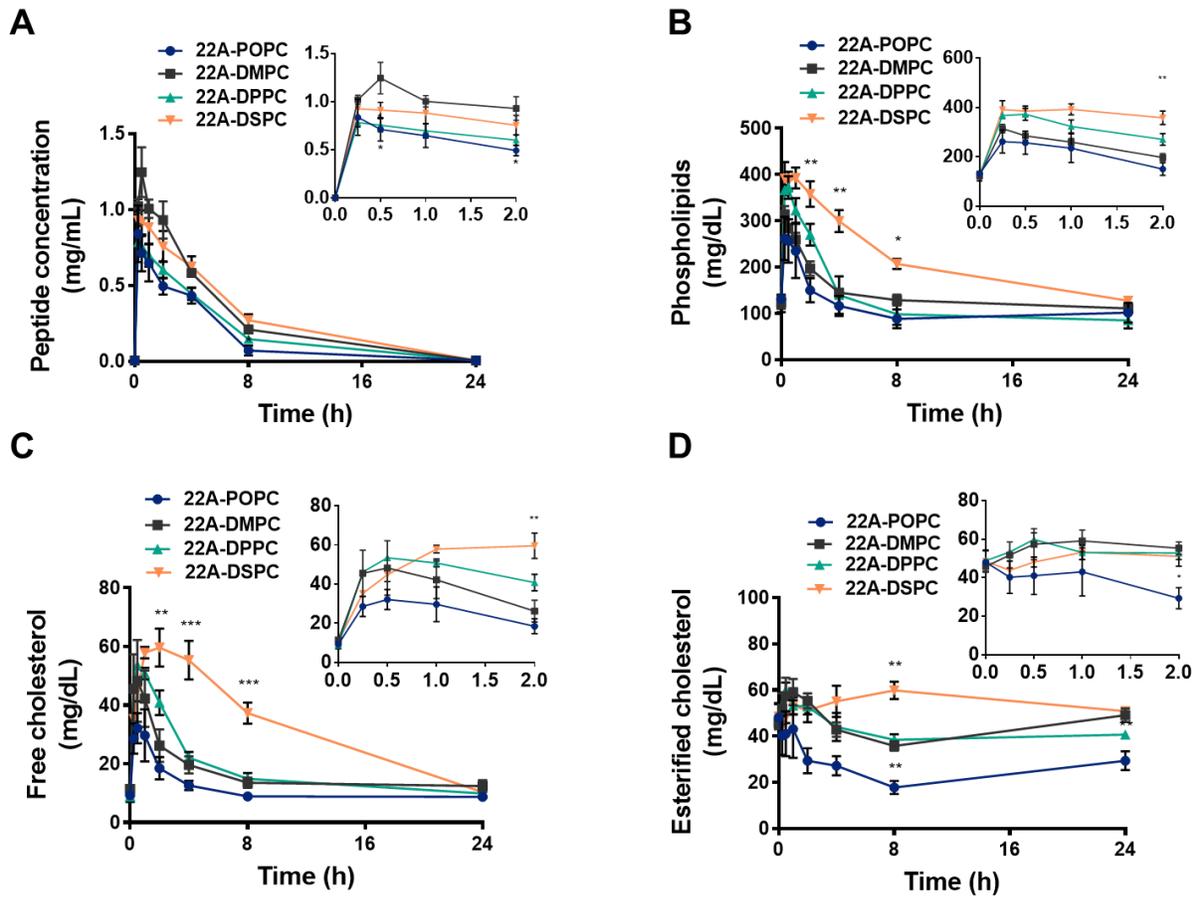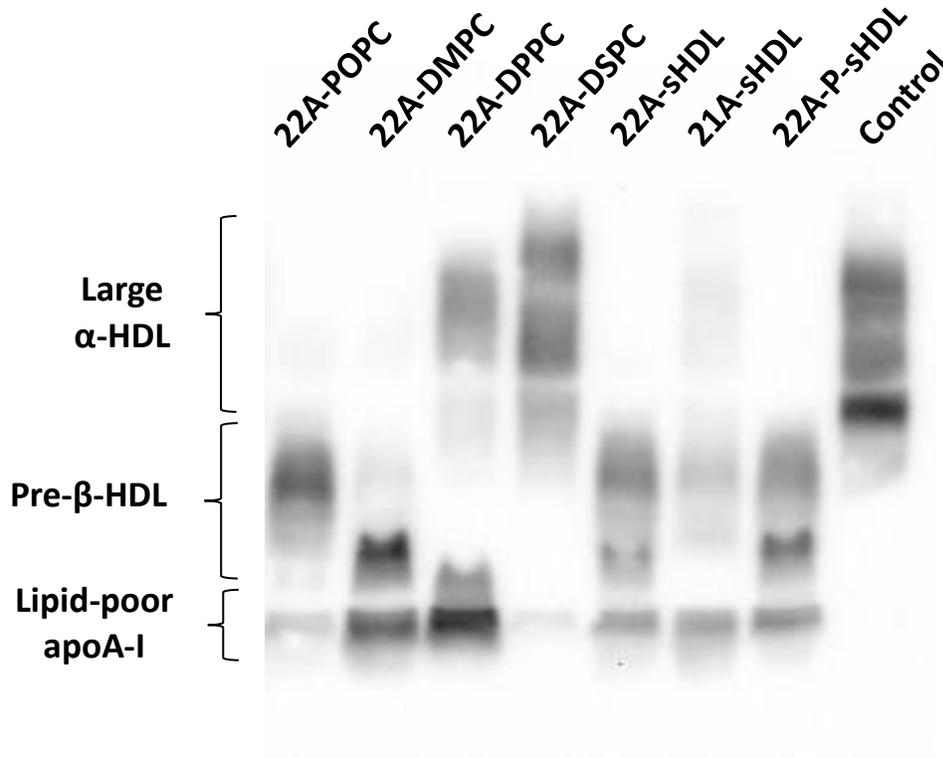**Figure 3**

Figure 4

Figure 5

Figure 6

Supplemental data

Title: Phospholipid component defines pharmacokinetic and pharmacodynamic properties of synthetic high-density lipoproteins

Authors: Maria V. Fawaz[1*], Sang Yeop Kim[2*], Dan Li[2], Ran Ming[2], Ziyun Xia[2], Karl Olsen[2], Irina D. Pogozheva[1], John J. G. Tesmer[3] and Anna Schwendeman[2,5**]

*Denotes equal contribution

[1]Department of Medicinal Chemistry, College of Pharmacy, University of Michigan, Ann Arbor, MI 48109

[2]Department of Pharmaceutical Sciences, College of Pharmacy, University of Michigan, Ann Arbor, MI 48109

[3]Department of Biological Sciences, Purdue University, West Lafayette, IN 47907

[5]Biointerfaces Institute, University of Michigan, Ann Arbor, MI 48109

Journal title: The Journal of Pharmacology and Experimental Therapeutics (JPET)

Name	Particle Size (nm)[a]	Retention Time (min)[b]	Purity (%)[c]	Impurity (%)[c]	
				Free Peptide	Liposome
22A-DMPC	10.1 ± 3.3	8.0	98.5	1.1	0.4
21A-DMPC	9.9 ± 3.4	7.8	99.4	0.6	0.0
22A-P-DMPC	10.5 ± 3.6	7.6	98.2	1.8	0.0
22A-POPC	10.4 ± 3.9	8.2	98.0	0.9	1.1
22A-DMPC	8.3 ± 1.9	8.1	99.1	0.9	0.0
22A-DPPC	9.2 ± 2.3	8.0	98.8	0.9	0.3
22A-DSPC	9.9 ± 2.5	7.8	99.2	0.8	0.0

Supplemental Table 1. Characterization of sHDL particles prepared with different peptides and phospholipids. [a]Particle size of sHDL measured by DLS; [b]Retention time of sHDL particle measured by GPC; [c]Purity and impurity of sHDL determined by area under the curve from GPC.

Name	V_{max} (µM/h)	K_m (µM)	R square
22A-DMPC	43.2 ± 4.9	14.5 ± 3.6	0.97
21A-DMPC	16.8 ± 10.1	32.0 ± 31.8	0.80
22A-P-DMPC	33.4 ± 3.6	7.1 ± 2.2	0.93
22A-POPC	35.7 ± 1.7	11.0 ± 1.5	0.97
22A-DMPC	11.9 ± 3.0	22.2 ± 12.1	0.84
22A-DPPC	Ambiguous	Ambiguous	Ambiguous
22A-DSPC	Ambiguous	Ambiguous	Ambiguous

Supplemental Table 2. Michaelis-Menten parameters of sHDL particles prepared with different peptides and phospholipids.